Anomalous properties in the normal and superconducting states of $LaRu_3Si_2$

Sheng Li,[1] Bin Zeng,[2] Xiangang Wan,[1] Jian Tao,[1] Fei Han,[2] Huan Yang,[1] Zhihe Wang,[1] and Hai-Hu Wen[1,*]

[1]*Center for Superconducting Physics and Materials, National Laboratory of Solid State Microstructures and Department of Physics, Nanjing University, Nanjing 210093, China*

[2]*Institute of Physics and Beijing National Laboratory for Condensed Matter Physics, Chinese Academy of Sciences, P.O. Box 603, Beijing 100190, China*

(Received 11 November 2011; published 29 December 2011)

Superconductivity in $LaRu_3Si_2$ with the Kagome lattice of Ru has been investigated. It is found that the normal-state specific heat C/T exhibits a deviation from the Debye model down to the lowest temperature. This may be induced by the existence of some high-frequency phonon modes or by the electron correlation effect. A relation $C/T = \gamma_n + \beta T^2 - AT\ln T$ which concerns the electron correlations can fit the data very well. The suppression to the superconductivity by the magnetic field is not the mean-field type, which is associated well with the observation of strong superconducting fluctuations. The field dependence of the induced quasiparticle density of states measured by the low-temperature specific heat shows a nonlinear feature, indicating the significant contributions given by the delocalized quasiparticles. The Wilson ratio determined for this material is about 2.88, indicating also a strong correlation effect.

DOI: 10.1103/PhysRevB.84.214527 PACS number(s): 74.70.Dd, 74.10.+v, 74.25.Bt, 74.25.F−

I. INTRODUCTION

Superconductivity arising from non-phonon-mediated pairing, such as through exchanging the magnetic spin fluctuations, has renewed interests in condensed-matter physics. The superconducting (SC) mechanism of the cuprates[1] and the iron pnictides,[2] although not yet settled completely, should have a close relationship with the electron correlations.[3–5] A similar assessment may extend to many others, like heavy fermion[6] and organic materials.[7] In this regard, the systems RT_3Si_2 or RT_3B_2 (R stands for the rare-earth elements, like La, Ce, Y, etc., T for the transition metals, like Ru, Co, and Ni, etc.) provide an interesting platform, since a variety of combinations of chemical compositions allow the system to be tuned between SC and magnetic, and sometimes both phases coexist.[8,9] Among these samples, the $LaRu_3Si_2$ has a SC transition temperature as high as 7.8 K.[10] As shown by Fig. 1, the material of $LaRu_3Si_2$ contains layers of Ru with the Kagome lattice sandwiched by the layers of La and Si, forming a $P6_3/m$ or $P6_3$ space group. Interestingly the La atoms construct a triangle lattice, while the Si atoms form a honeycomb structure. The electric conduction is strongly favored by the Ru chains along the z axis (as evidenced by our band structure calculations). Preliminary experiment found that the SC transition temperature drops only 1.4 K with the substitution of 16% La by Tm (supposed to possess a magnetic moment of about $8\mu_B$), suggesting that the superconductivity is robust against the local paramagnetic moment.[8] By doping the La sites with Gd, a coexistence of superconductivity and the spin glass state[11] was observed. In $CeRu_3Si_2$, the SC transition temperature drops to about 1 K and a valence fluctuation model was proposed for the pairing.[12] Since the Ru atom locates just below the Fe in the periodic table, a key player in the iron pnictide superconductors, therefore it is very curious to know whether the superconductivity here is induced by the electron-phonon coupling or by other novel mechanism, such as the electron correlations. In this paper we report the results of transport and specific heat on samples of $LaRu_3Si_2$. Our results reveal some novelties in both the SC and normal states of $LaRu_3Si_2$.

II. EXPERIMENTAL METHODS AND CHARACTERIZATION

The samples were fabricated by the arc melting method.[8,10,11] The starting materials—La metal pieces (99.9%, Alfa Aesar), Ru powder (99.99%), and Si powder (99.99%)—were weighed and mixed well and pressed into a pellet in a glover box filled with Ar atmosphere (water and the oxygen compositions were below 0.5 ppm). In order to avoid the formation of the $LaRu_2Si_2$ phase, we intentionally let a small amount of extra Ru with the nominal compositions as $LaRu_{3+x}Si_2$. Three rounds of welding with the alternative upper and bottom on the pellet were taken in order to achieve the uniformity. After these refined processes, the resultant sample contains mainly the phase of $LaRu_3Si_2$ and a small amount of Ru remains as the impurity phase. In Fig. 2 we plot the x-ray diffraction (XRD) patterns on one typical sample and the Rietveld fitting using the GSAS program. It is clear that the main diffraction peaks can be indexed well by a hexagonal structure with $a = 5.68$ Å and $c = 3.565$ Å. Some weak peaks arising from the impurity phase Ru can also be seen. A detailed fitting to the structural data find that the ratio between $LaRu_3Si_2$ and Ru is around 85:15 for this typical sample. The sample preparation and the quality characterized by the SC transitions can be repeated quite well. It is found that some of the $LaRu_2Si_2$ phase with a tetragonal structure can be found if the starting material has the nominal composition of $LaRu_3Si_2$. In this case, the XRD data exhibit clearly two sets of structures and can be easily indexed by the GSAS program. For the present sample, the absolute difference between the experimental data and the fitting curve can be observed for some peaks because part of the grains in the sample are slightly aligned. The resistivity was measured with a Quantum Design instrument PPMS-16T with a standard four-probe

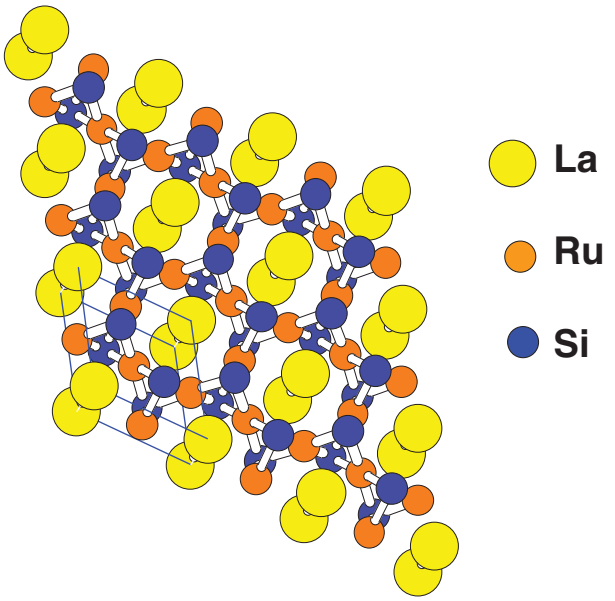

FIG. 1. (Color online) The atomic structure of $LaRu_3Si_2$. The Ru atoms construct a Kagome lattice, while the Si and La atoms form a honeycomb and a triangle structure, respectively. The three different atoms do not overlap each other from a top view. The prism at the bottom left corner illustrates one unit cell of the structure.

technique, while the magnetization was detected by the Quantum Design instrument SQUID-VSM with a resolution of about 5×10^{-8} emu.

III. RESULTS AND DISCUSSION

A. Resistive and magnetization

In Fig. 3(a) we present the temperature dependence of magnetization measured in the zero-field-cooling (ZFC) mode

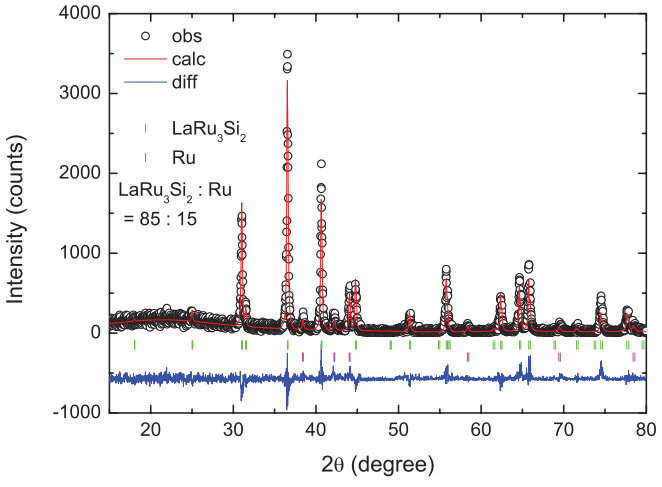

FIG. 2. (Color online) X-ray diffraction patterns of the sample $LaRu_3Si_2$. All main diffraction peaks can be indexed well by a hexagonal structure with $a = 5.68$ Å and $c = 3.565$ Å with Ru as the impurity phase. For some peaks the difference between the data and the fitting is a bit large because some of the grains of the polycrystalline sample are slightly oriented. The ratio between $LaRu_3Si_2$ and Ru is found to be 85:15.

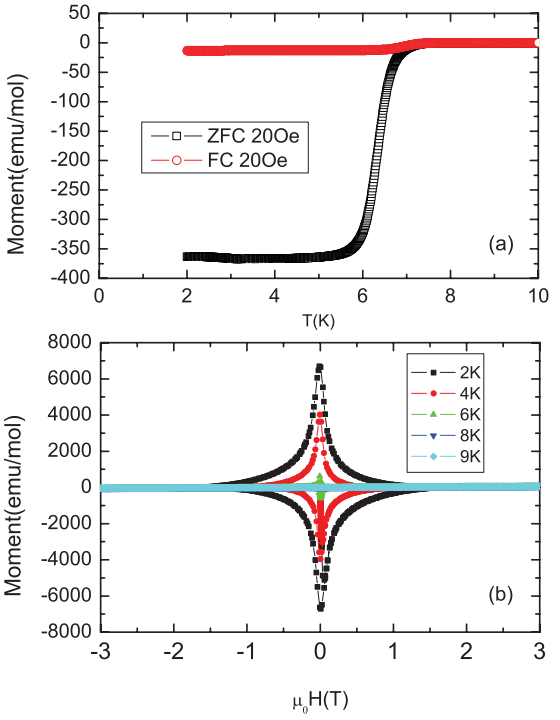

FIG. 3. (Color online) (a) Temperature dependence of the dc magnetization measured in the ZFC mode and the FC mode at a magnetic field of 20 Oe. (b) The MHLs measured with a field sweeping rate of 50 Oe/s at different temperatures. At 9 K, the MHL shows a rough linear paramagnetic behavior.

and the field-cooling (FC) mode. By considering the demagnetization factor on the ZFC data, the Meissner screening is estimated to be almost 100%. This indicates that the SC connections between the grains of $LaRu_3Si_2$ are very good, although we have a slight secondary phase of Ru. The onset T_c determined from the magnetization is around 7.8 K. The majority of the SC transition occurs at about 6.6 K under a magnetic field of 20 Oe. This difference is not induced by the inhomogeneity of the sample; it may be induced by the relatively strong SC fluctuations (see below). Figure 3(b) shows the magnetization hysteresis loops (MHLs) measured at different temperatures. The symmetric and clear opening of the MHLs indicates that it is a type II superconductor. A roughly linear MHL was observed at 9 K, just above T_c, indicating that the normal state has no long-range ferromagnetic order. We did not observe a magnetization enhancement near T_c, which was reported in Tm- and Gd-doped samples in early publications.[8,11] Figure 4(a) shows the resistive transitions at zero field (main panel) and different magnetic fields under 4 T (inset). The onset resistive transition temperature is at 7.9 K (95% normal state resistivity ρ_n), and the zero resistivity was achieved at about 6.8 K. By applying a magnetic field, the resistive transition broadens. Taking different criterions of resistivity we determined the upper critical field $H_{c2}(95\%\rho_n)$, $H_{c2}(50\%\rho_n)$, and the irreversibility line $H_{\rm irr}(0.1\%\rho_n)$. It is clear that there is a large difference between the $H_{c2}(95\%\rho_n)$ and $H_{\rm irr}(T)$. We argue that this may be induced by the strong SC fluctuations.

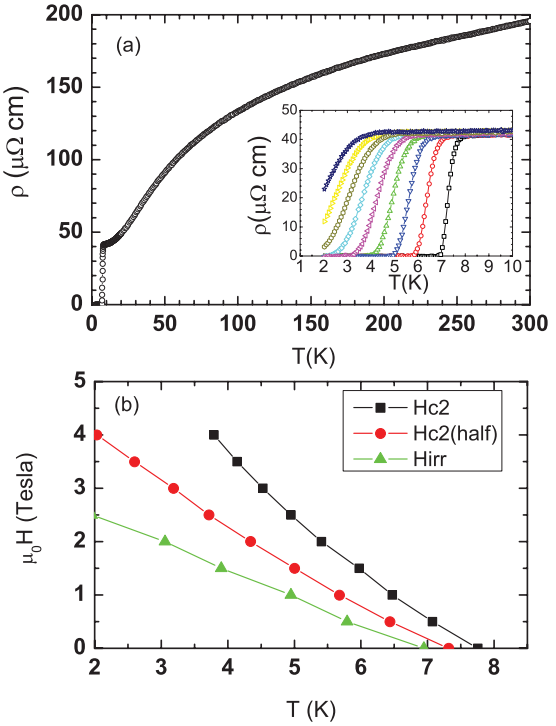

FIG. 4. (Color online) (a) Temperature dependence of resistivity at zero magnetic field. The inset shows the resistivity at different magnetic fields: 0, 0.5, 1.0, 1.5, 2.0, 2.5, 3.0, 3.5, and 4.0 T. (b) Temperature dependence of the critical magnetic field with three different criterions: H_{c2} (squares, 95%ρ_n), H_{c2} (circles, 50%ρ_n), and the irreversibility line $H_{\rm irr}$ (up triangles, 0.1%ρ_n). There is a large area between the H_{c2} (95%ρ_n) and $H_{\rm irr}$ (0.1%ρ_n), which is probably induced by the strong SC fluctuation.

B. Specific heat

The raw data of specific heat was shown in Fig. 5(a). A SC anomaly appears at about 7.6 K. Since the Ru has a SC transition at 0.49 K and a quite small normal-state specific heat coefficient ($\gamma_n^{\rm Ru} = 2.8$ mJ/mol K^2), a slight correction of about 0.47 mJ/mol K^2 was made to the data. By applying a magnetic field, the SC anomaly shifts to lower temperatures. It is interesting to note that the transition is not shifted parallel down to the low temperatures (the so-called mean-field type), rather the SC anomaly is suppressed and becomes wider and wider. One may argue that this progressive widening of the specific anomaly is due to the possible impurity phase of the Ru, as argued in the superconductor with a nodal gap.[13,14] While since both the resistive and the specific heat anomaly at zero field is rather sharp, we would not believe this effect is induced by the Ru impurity, which, to our understanding, act as nonmagnetic scattering centers. Actually, this kind of field-induced broadening was clearly seen in the cuprate superconductor $Pr_{0.88}LaCe_{0.12}CuO_{4-\delta}$[15] and was ascribed to a strong SC fluctuation. Combining this fact with the broadened resistive transitions under magnetic fields, we would argue that there is also a strong SC fluctuation in $LaRu_3Si_2$. As for a three-dimensional system judged from our band structure calculations, this kind of strong SC fluctuation may suggest that the superfluid density may be low.

Another interesting point shown in Fig. 5(a) is that the normal state-specific heat (SH) coefficient C/T shows a nonlinear dependence on T^2 down to the lowest temperature (0.38 K). This is clearly deviating from the prediction of the Debye model. Taking the slope of C/T vs T^2 from the low-temperature data, we get the Debye temperature $T_D = 284$ K. The phonon contribution calculated based on the Debye model $C_{\rm Debye} \propto (T/T_D)^3 \int_0^{T_D/T} [e^4 e^x/(e^x-1)^2] dx$ is shown by the red dashed line. One can see that the Debye model is seriously violated. We should emphasize that this deviation is not induced by the Ru impurity phase, since a simple estimate finds that 15% Ru impurity in the material gives only about 2.5% of the total phonon contribution of the sample.[16] This violation may have two different reasons: One assumes that there are some unique high-frequency phonon modes, which makes the Debye model invalid; another one is due to the electron correlation effect. We give further discussions below.

If some high-frequency phonon modes are present, the specific heat may be expressed as

$$C/T = \gamma_n + \beta T^2 + \eta T^4 \qquad (1)$$

(or to include even higher terms $C/T = \gamma_n + \beta T^2 + \eta T^4 + \delta T^6$), with the last two or three terms coming from the phonon contributions. This kind of treatment was done in many unconventional superconductors by Yang *et al.*[17] By fitting our data to the former equation, we indeed get a good fit, as shown in Fig. 6, yielding $\gamma_n = 36.8$ mJ/mol K^2, $\beta = 0.1467$ mJ/mol K^4, and $\eta = 0.00465$ mJ/mol K^6. Using the value of β and the relation $\Theta_D = (12\pi^4 k_B N_A Z/5\beta)^{1/3}$, where $N_A = 6.02 \times 10^{23}$ mol^{-1} is the Avogadro constant, $Z = 6$, is the number of atoms in one unit cell, we get the Debye temperature $\Theta_D \approx 412$ K. If this interpretation is correct, the large difference of the experimental data and the Debye model should find a theoretical base for some unique high-frequency phonon modes.

Alternatively, it is naturally questioned whether this violation is induced by some electron correlation effect. For a non-Fermi liquid with three dimensionality, the enhanced electron-electron interaction will give an extra contribution to the electronic specific heat[18] $C_{e-e} = -AT^n \ln T$ with $n = 1$ to 3. Thus, we fit the data with the relation

$$C = \gamma_n T + \beta T^3 - AT^n \ln T. \qquad (2)$$

The last term gives the correction to the Fermi liquid description, $n = 1$ corresponds to the case of strong correlation, like in Heavy fermion systems,[18] while $n = 3$ corresponds to a weak correlation. Using above equation and $\gamma_n = 36.8$ mJ/mol K^2, we found a much better fitting when n takes 2, as shown by the solid line, leading to $\beta = 1.416$ mJ/mol K^4 and $A = 3.61$ mJ/mol K^3. Therefore, we intend to conclude that the electron correlations may play an important role in the system. In Fig. 5(b), we derived the electronic specific heat by subtracting the normal-state background measured at 5 T. One can see that the low-T part of C_e/T exhibits a flat feature, indicating a full SC gap. There is a small upturn of C_e/T in the low-T region when the field is very weak (see the data of 0.25 and 0.5 T), which is attributed to the Schotkky anomaly

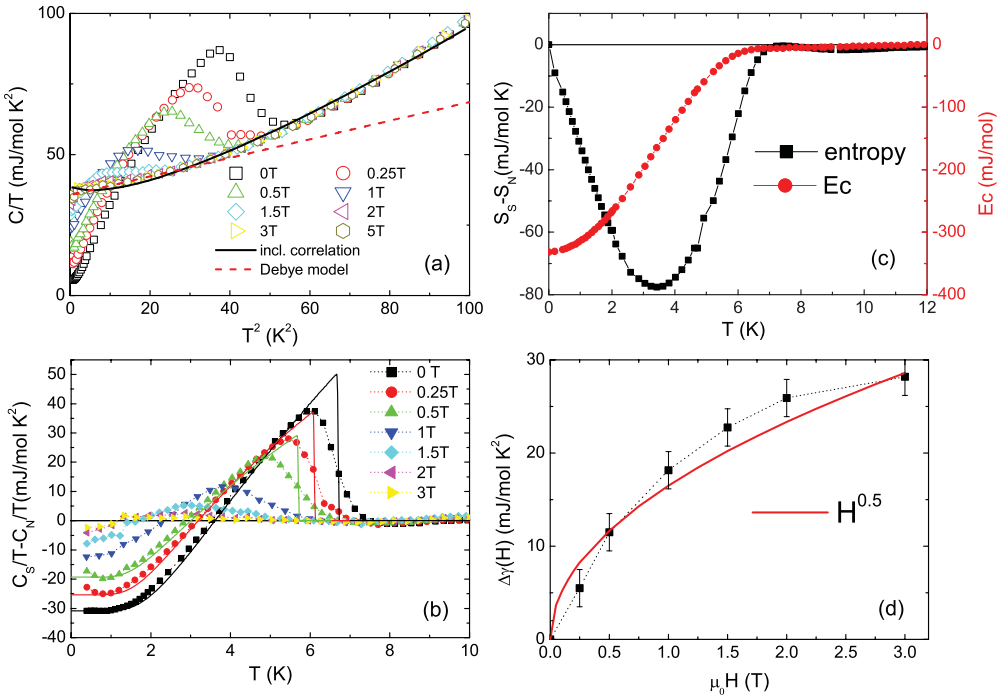

FIG. 5. (Color online) (a) The raw data of specific heat coefficient C/T vs T^2, at different magnetic fields ranging from 0 to 5 T. The normal state data (at 5 T) shows a nonlinear feature down to the lowest temperature here, indicating a deviation from the Debye model, as shown by the red dashed line. The solid line represents the fit to the formula including the electron correlations (see text). (b) The electronic specific heat coefficient obtained by subtracting normal state value C_N/T (data at 5 T) from the total. The solid lines are the theoretical fitting curves based on the BCS model. (c) The entropy difference (squares) between the SC state and the normal state, derived from $S_S - S_N = \int_0^T (C_S/T' - C_N/T')dT'$ at zero field and 5 T. The condensation energy is calculated by $E_c = \int_0^T (S_S - S_N)dT'$. (d) The magnetic field dependence of the field induced electronic specific heat $\Delta\gamma(H)$. The nonlinear field dependence is very clear. The red solid line is a fit to the $\sqrt{H}$.

due to the paramagnetic centers. Using an integral based on the BCS formula for electronic specific heat,

$$\gamma_e = \frac{4N(E_F)}{k_B T^3}\int_0^{+\infty}\int_0^{2\pi}\frac{e^{\zeta/k_BT}}{(1+e^{\zeta/k_BT})^2} \times\left(\varepsilon^2+\Delta^2(\theta,T)-\frac{T}{2}\frac{d\Delta^2(\theta,T)}{dT}\right)d\theta\,d\varepsilon, \quad (3)$$

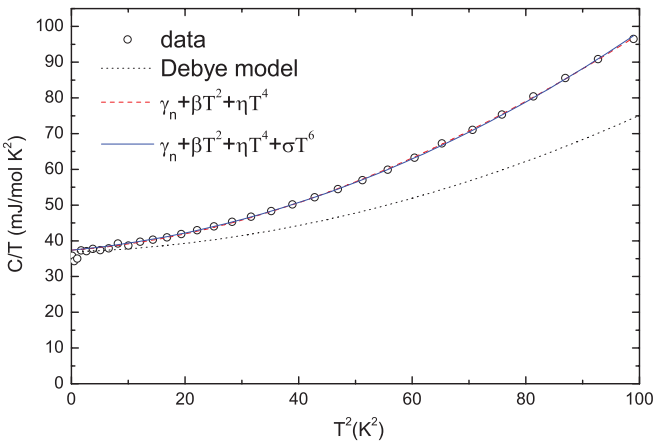

FIG. 6. (Color online) The raw data of specific heat coefficient C/T vs T^2 5 T, together with the fitting of three different models (see text).

where $\zeta = \sqrt{\varepsilon^2 + \Delta^2(T,\theta)}$ and $\Delta(T,\theta) = \Delta_0(T)$ for the s-wave symmetry, we fit the data at $\mu_0 H = 0$, 0.25, and 0.5 T and show them with the solid lines. In this way we obtained the data in the zero temperature limit for each field. For higher magnetic fields, it is known that the Schottky anomaly becomes weaker; we can determine the low-T data directly from the experimental data. Figure 5(c) shows the temperature dependence of the entropy calculated using $S = \int_0^T C_e/T'dT'$; it is clear that the entropy is conserved at T_c as judged by $S_S - S_N|_{T_c} = 0$, where S_S or S_N are the entropies of the SC state and the normal state integrated up to T, and $S_S - S_N = \int_0^T (C_S/T' - C_N/T')dT'$. After obtaining the low-T data, we derived the electronic SH at different magnetic fields and plot them in Fig. 5(d). Interestingly, a nonlinear field dependence can be easily seen here. Further analysis finds that this nonlinear dependence is actually different from the $\sqrt{H}$ relation [shown by the solid line in Fig. 5(d)] predicted for a clean superconductor with line-node gap; the data below about 0.5 T seem to be more linear. Our result here is certainly different from a linear relation as predicted for a single isotropic SC gap. A multigap feature would already explain the data, but as seen from the flattening of C_e/T at $T \to 0$, we would argue that it is not the multigap feature, but the gap anisotropy that leads to the nonlinear field dependence of C_e/T. A momentum resolved measurement is highly desired to uncover this puzzle.

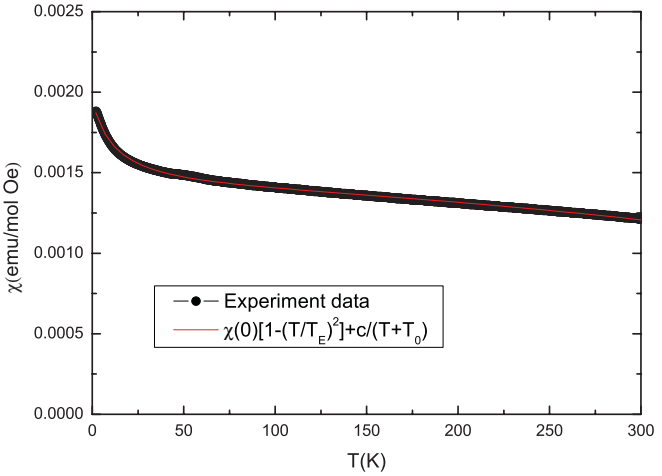

FIG. 7. (Color online) Temperature dependence of the magnetic susceptibility measured at 5 T. The solid line is a fit to the theoretical curve, namely, Eq. (5).

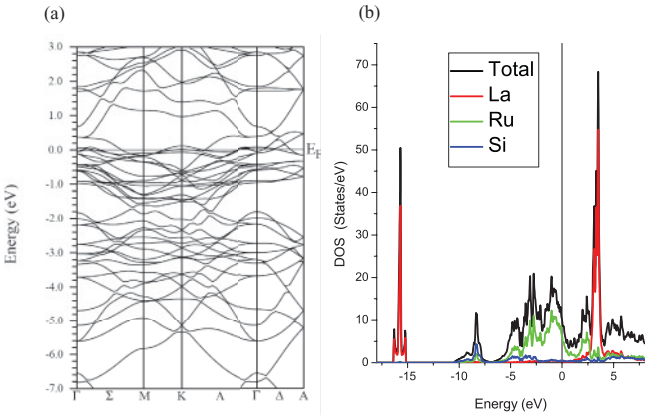

FIG. 8. (Color online) (a) The energy bands obtained from the DFT calculations. The dense bands near E_F are derived from the Ru 4d orbitals. (b) The electronic density states from the band structure calculations. It is found that the DOS at the E_F are mainly contributed by the Ru orbitals. The DOS from the La and the Si atoms at E_F are negligible.

C. Wilson ratio

In order to know how strong the electron correlation effect is in the material, we measured the magnetic susceptibility of the material and calculate the Wilson ratio.[19] The data is shown in Fig. 7 together with the fitting curve. In a Fermi liquid, the Wilson ratio is defined as

$$R = \frac{4\pi^2 k_B^2}{3(g\mu_B)^2}\frac{\chi(0)}{\gamma_n}, \tag{4}$$

which measures the correlation strength; here $\chi(0)$ is the Pauli susceptibility arising from the electronic origin, which should be roughly temperature independent, γ_n is the specific heat coefficient, g is Lande factor which takes about 2 for an electron, and μ_B is the Bohr magneton. The Wilson ratio is a dimensionless quantity, which is about 1 for the noninteracting electron gas and about 1–2 for interacting Fermi liquid. When R is larger than 2, the correlation effect is strong. In a real material, the magnetic susceptibility can arise from several possible reasons. For a system with long-range magnetic order, it may have two origins: the Pauli term and the ionic (orbital and the nuclei) term, assuming the total magnetic susceptibility is

$$\chi(T) = \chi(0)\left[1 - \left(\frac{T}{T_E}\right)^2\right] + \frac{c}{T + T_0}. \tag{5}$$

The first term is coming from the Pauli susceptibility corrected with a temperature dependence of the density of states at the Fermi energy. The T_E is a parameter proportional to the Fermi energy. The second term is related to some weak magnetism arising probably from the ionic contributions. By fitting to the data we get $\chi(0) = 0.00144$ emu/mol Oe, $T_E = 702$ K, $c = 0.004$ emu K/mol Oe, and $T_0 = 7$ K. Using $\gamma_n = 36.8$ mJ/mol K^2, it is found that the Wilson ratio $R = 2.88$, which is much larger than 1, indicating a strong electron correlation effect.

D. Density-functional theory calculations

To have a comprehensive understanding on the properties of $LaRu_3Si_2$, we did the density-functional theory calculations by using the WIEN2K package[20] utilizing the generalized gradient approximation[21] for the exchange-correlation potential. As shown in Fig. 8(a), the bands around Fermi level are mainly contributed by Ru 4d. The Si 3p bands are very wide and have some hybridization with Ru 4d. Further analysis of the calculation shows that the crystal-field splitting upon Ru 4d orbitals is quite weak, consequently all Ru 4d electron should play a role in conduction and related superconductivity. There are several bands crossing the Fermi level, which leads to complicated 3D Fermi surfaces; this will be presented elsewhere. Since the band closed to the Fermi level is narrow the density of states (DOS) at the Fermi level is high, as shown in Fig. 8(b). We also perform spin-polarized calculations to check the possible magnetic instability. The calculation shows that the ferromagnetism is not stable for this compound. We cannot find any strong nesting effect in the Fermi-surface; thus, the spin-density wave order is unlikely. Worthy of noting is that all the five Ru 4d orbitals contribute to the conduction in $LaRu_3Si_2$, which is very similar to the case of the iron in the iron-pnictide superconductors.[22] Actually a Ru-based compound, namely, $LaRu_2P_2$, is a superconductor with $T_c = 4.1$ K, which has the similar structure of the $BaFe_{2-x}Co_xAs_2$ superconductor,[23,24] and probably the same SC mechanism. This reminds us that the correlation effect may play some roles in the superconductivity of $LaRu_3Si_2$.

IV. SUMMARY

In summary, resistivity, magnetization and specific heat have been measured in a Ru-based superconductor $LaRu_3Si_2$ with T_c of about 7.8 K. The temperature dependence of the specific heat coefficient C/T deviates clearly from the Debye model. This deviation can be either explained as the effect of some unique high-frequency phonon mode or indicates the possible evidence of electron correlations. The SC transitions measured by both resistivity and specific heat self-consistently present the evidence of strong SC fluctuations, resembling that in the cuprates. The field induced quasiparticle density of states

show a nonlinear magnetic field dependence, which is argued as a gap anisotropy. The Wilson ratio determined is about 2.88. Combining the novelties found both in the normal state and the SC state, we argue that the electron correlations may play an important role in the occurrence of superconductivity in $LaRu_3Si_2$.

ACKNOWLEDGMENTS

We appreciate the useful discussions with Jan Zaanen, Zidan Wang, Zlatko Tesanovic, Tao Xiang, Qianghua Wang, and Jianxin Li. This work is supported by the NSF of China, the Ministry of Science and Technology of China (973 projects: 2011CBA00102), and the Chinese Academy of Sciences.

*hhwen@nju.edu.cn

[1] J. G. Bednorz and K. A. Muller, Z. Phys. B **64**, 189 (1986).

[2] Y. Kamihara *et al.*, J. Am. Chem. Soc. **130**, 3296 (2008).

[3] P. W. Anderson *et al.*, J. Phys. Condens. Matter **16**, R755 (2004).

[4] D. J. Scalapino, Phys. Rep. **250**, 329 (1995); T. Moriya and K. Ueda, Rep. Prog. Phys. **66**, 1299 (2003); P. Monthoux, D. Pines, and G. Longarich, Nature (London) **450**, 20 (2007).

[5] N. Ni, M. E. Tillman, J. Q. Yan, A. Kracher, S. T. Hannahs, S. L. Budko, and P. C. Canfield, Phys. Rev. B **78**, 214515 (2008).

[6] Q. M. Si and F. Steglich, Science **329**, 1161 (2010).

[7] M. Dressel *et al.*, J. Phys. Condens. Matter **23**, 293201 (2011).

[8] M. Escorne, A. Mauger, L. C. Gupta, and C. Godart, Phys. Rev. B **49**, 12051 (1994).

[9] H. C. Ku *et al.*, Solid State Commun. **35**, 91 (1980).

[10] H. Barz, Mater. Res. Bull. **15**, 1489 (1980); J. M. Vandenberg and H. Barz, *ibid.* **15**, 1493 (1980).

[11] C. Godart and L. C. Gupta, Phys. Lett. **120**, 427 (1987).

[12] U. Rauchschwalbe, W. Lieke, F. Steglich, C. Godart, L. C. Gupta, and R. D. Parks, Phys. Rev. B **30**, 444 (1984).

[13] Grzegorz Haran, Jason Taylor, and A. D. S. Nagi, Phys. Rev. B **55**, 11778 (1997).

[14] Leonid A. Openov, Phys. Rev. B **69**, 224516 (2004).

[15] S. D. Wilson *et al.*, Proc. Natl. Acad. Sci. USA **104**, 15259 (2007).

[16] W. Reese and W. L. Johnson, Phys. Rev. B **2**, 2972 (1970).

[17] H. D. Yang and J.-Y. Lin, J. Phys. Chem. Solids **62**, 1861 (2001).

[18] H. v. Loehneysen, A. Rosch, M. Vojta, and P. Woelfle, Rev. Mod. Phys. **79**, 1015 (2007).

[19] K. G. Wilson, Rev. Mod. Phys. **47**, 773 (1975).

[20] P. Blaha, K. Schwarz, G. Madsen, D. Kvasicka, and J. Luitz, WIEN2K, An Augmented Plane Wave + Local Orbitals Program for Calculating Crystal Properties (Technical University of Vienna, Vienna, 2001).

[21] J. P. Perdew, K. Burke, and M. Ernzerhof, Phys. Rev. Lett. **77**, 3865 (1996)

[22] D. J. Singh and M. H. Du, Phys. Rev. Lett. **100**, 237003 (2008).

[23] A. S. Sefat, R. Jin, M. A. McGuire, B. C. Sales, D. J. Singh, and D. Mandrus, Phys. Rev. Lett. **101**, 117004 (2008).

[24] S. L. Bud'ko, Ni Ni, and P. C. Canfield, Phys. Rev. B **79**, 220516 (2009).